

# Model Representations of the Interaction Between the Solar Wind and the Supersonic Interstellar Medium Flow. Prediction and Interpretation of Experimental Data

V. B. Baranov and V. V. Izmodenov

Received December 5, 2005

**Abstract** — The planning and conducting of physical experiments requires the development of theoretical models capable either of predicting possible experimental data or explaining those already obtained. The processes taking place in the physical world can be understood only in terms of the close interaction between theory and experiment. Developing any quantitative or qualitative model of a physical phenomenon requires a mathematical apparatus, on the basis of which such models can be constructed. The branch of theoretical science using the methods of magnetohydrodynamics and hydroaeromechanics for studying space physics problems is usually called cosmic gasdynamics; it is mostly used in developing models of physical phenomena occurring under space conditions.

In order to emphasize the importance of cosmic gasdynamics in the development of astrophysics and space research, we will present several examples of models constructed by aerodynamicists. These models not only played an important role in qualitative predictions but are still being developed due to the need for the quantitative interpretation of the experimental data.

The solar corona was long thought to be a formation in a state of gravitational equilibrium (Chapman model). However, it turned out that the pressure at infinity obtained on the basis of this equilibrium solution is considerably greater than the estimated pressure in the interstellar gas surrounding the solar corona. In [1] it was concluded that in this case the solar corona gas must expand and a solution describing this expansion was obtained by invoking the steady-state hydrodynamics equations in the spherically-symmetric approximation. The solution of these equations led to the theoretical prediction of the solar wind, a radial flow of fully ionized hydrogen plasma issuing from the solar corona at a low subsonic velocity but already hypersonic at the Earth's orbit. Subsonic-to-supersonic transition is ensured by solar gravitation which in this case plays the role of a convergent-divergent nozzle. Within a year, the theoretical prediction of the solar wind [1] was confirmed by its experimental detection [2] onboard the Soviet spacecraft *Luna-2*. It turned out that at the Earth's orbit the mean velocity of the solar wind  $V_E \approx 450 \text{ km}\cdot\text{s}^{-1}$ , the mean proton temperature  $T_E \approx 6 \cdot 10^4 \text{ K}$  (the electron temperature is somewhat higher), and the mean concentration of protons (and electrons)  $n_E \approx 10 \text{ cm}^{-3}$ .

The first hydrodynamic model of the supersonic solar-wind flow past the Earth's magnetosphere [3] was only qualitative, since it considered a flow past a plane magnetic dipole in the approximation of a thin layer between the bow shock and an "obstacle" embedded in the flow. However, it was constructed before the actual discovery of the solar wind and provided further important impetus to the development of models of the supersonic solar wind flow past planets with a detached shock.

One more example is furnished by the gasdynamic model of the solar wind flow past cometary atmospheres, first suggested in [4]. A complete numerical solution of the problem formulated in that study was obtained almost twenty years later [5]. Many results obtained in [5] were later confirmed by experiments to investigate the P/Halley comet performed during the flyby of the spacecraft *Vega 1* and 2, *Giotto*, *Suisei*, and *Sakigake* in 1986.

In this work, a model of the interaction between the supersonic solar wind and the supersonic flow of the local, i.e., surrounding the Sun, interstellar medium is considered; it was first suggested in [6] in a much simplified formulation. This model has been actively developed in connection with the flights of the spacecraft *Voyager 1* and 2, *Ulysses*, *Hubble Space Telescope*, *SOHO*, and others, exploring the outer regions of the solar system.

**Keywords:** solar wind, local interstellar medium, shock wave, heliopause, kinetic-gasdynamic model, resonance charge-exchange, Monte Carlo method, heliospheric interface.

## 1. GENERAL MODEL REPRESENTATIONS OF THE INTERACTION BETWEEN THE SOLAR WIND AND THE LOCAL INTERSTELLAR MEDIUM

An impetus to the construction of a model of the interaction between the supersonic solar wind and the supersonic flow of the local interstellar medium [6] was given, first, by the results [1], which led to a constant radial velocity of the solar wind up to infinity, this being in contradiction with a finite pressure of the interstellar gas at rest at a temperature  $T_\infty \approx 10^4$  K, and, second, by the fact that the Sun is in motion relative to the near stars at a velocity of about 20 km/s. If the interstellar gas moves relative to the solar system at the same velocity, then the hypersonic solar wind must interact with the supersonic flow of the interstellar medium. In [6] it was suggested that the local interstellar medium is fully ionized hydrogen plasma and its flow is hypersonic relative to the Sun. The first assumption made it possible to consider the problem within the framework of the continuum model (for charged particles the effective Knudsen number  $\text{Kn} = l/L \ll 1$ , where  $l$  is the mean free path and  $L$  is the scale length in the problem under consideration), while the second assumption enabled the problem to be solved in the Newtonian thin-layer approximation [7]. Within a year of the publication of [6], measurements of the backscattered solar radiation in the hydrogen Lyman- $\alpha$  line (wavelength 1216 Å) onboard the American satellite OGO-5 [8, 9] showed that the interstellar gas actually has a velocity of about 20 km/s relative to the Sun and that the velocity vector lies almost in the ecliptic plane rather than making an angle of  $53^\circ$  with the latter, as followed from observations of the Sun's motion relative to the near stars. Somewhat later [10] the data on the backscattered solar radiation at a wavelength of 584 Å indicated similar motion of the interstellar helium atoms.

These first results of measurements of the backscattered solar radiation were obtained for neutral atoms for which  $\text{Kn} \geq 1$ . In this case, the model of the flow past the solar system cannot be constructed within the framework of continuum mechanics. Moreover, the direction of the measured velocity indicated that the interstellar gas flow is due to its own motion rather than the motion of the Sun relative to the near stars. Thus, it turned out that the model [6] cannot be directly applied to the phenomenon under consideration, though it has stimulated the development of certain lines of inquiry in astrophysics.

For understanding the processes related with the motion of the local interstellar medium relative to the solar system, the data of ground-based astronomical observations [11] turned out to be very important. It was found that the Sun is embedded in a partially ionized local interstellar cloud moving relative to the solar system at a velocity  $V_\infty \approx 26$  km/s, its temperature being  $T_\infty = 7000$  K. Moreover, the velocity vector direction coincided with the measured data obtained in the experiments on the backscattered solar radiation.

The qualitative pattern of the flow resulting from the interaction between the fully ionized hydrogen plasma of the solar wind and the partially ionized hydrogen plasma of the local interstellar medium is presented in Fig. 1. In what follows, for the sake of brevity, the charged component will be called the "plasma component", as distinct from the neutral component representing the flow of H atoms (other atoms have almost no effect on the flow owing to their low concentration as compared with that of hydrogen atoms). Since for the basic process of H atom collisions associated with charge exchange with protons (resonance charge exchange) we have  $\text{Kn} \geq 1$ , the interstellar H atom motion cannot be described within the framework of continuum mechanics. The atoms penetrate from the local interstellar medium into the solar system across strong discontinuity surfaces and, exchanging charges with protons, exert an effect on the plasma component motion.

The entire flow region can be divided into four subdomains (Fig. 1), namely, the supersonic solar wind (1), the solar wind heated in the heliospheric shock wave (2), the plasma component of the interstellar medium heated in the bow shock (3), and its supersonic oncoming flow (4). Regions 2 and 3 are usually called the inner and outer interfaces, respectively. In each of regions 1 to 4 charge exchange leads to the formation of newborn H atoms, having the same parameters as the protons in these regions, and newborn

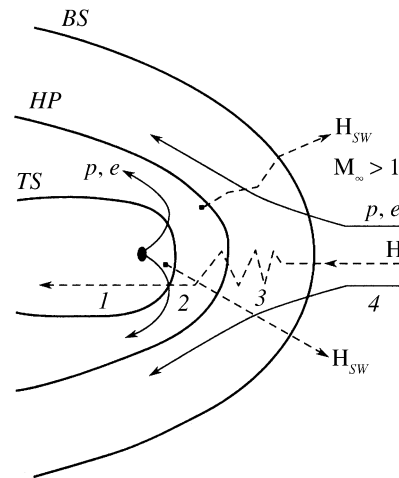


Fig. 1. Qualitative flow diagram; *HP* is the tangential discontinuity (heliopause) separating the fully ionized solar wind and the plasma component of the interstellar medium, *BS* is the bow shock, and *TS* is the heliospheric, or termination, shock across which the solar wind is decelerated. The broken lines denote the trajectories of the solar wind atoms  $H_{SW}$  (species 1 and 2) and the interstellar atoms (species 3 and 4)

protons with the parameters of neutral H atoms. The newborn protons are then “picked up” by the plasma component flows, thus altering the momentum and the energy of these flows. As a result of charge exchange, hydrogen atoms of at least three species are formed.

The trajectories of the  $H_{SW}$  hydrogen atoms born in regions 1 and 2 (atoms of types 1 and 2, respectively) are sketched in Fig. 1. These atoms with the parameters of the protons of regions 1 and 2 penetrate into the local interstellar medium and, exchanging charges with its protons, alter the parameters of the undisturbed flow ahead of the bow shock *BS*. The atoms of type 3 possess the same parameters as the interstellar medium protons in the outer interface while the atoms of the interstellar medium which penetrate into the solar system without charge exchange (primary atoms) will be called atoms of type 4.

As shown for the first time at the qualitative level in [12] and quantitatively in [13], it is the charge exchange between the hydrogen atoms from the interstellar medium and their own protons in the outer interface region that is most effective. As a result, the outer interface makes a good “filter” for hydrogen atoms penetrating into the solar system from the interstellar medium. In [13] it was shown that the assumption of a small interface thickness, as compared with its distance from the Sun, made in [16] does not hold for the actual parameters of the interacting flows.

The important role of the interface introduced in [6, 13] first gained the recognition of theoreticians in [12–14]. As for the experimentalists, up to 1985 in interpreting the backscattered solar radiation measured onboard many space vehicles, such as *Prognoz*, *Venera*, *Mars*, and others, they used the so-called “hot” model, in which there is no interface. In that model, the processes of resonance charge exchange between interstellar H atoms and solar wind protons, H atom photoionization, and the forces of solar gravitation and radiative repulsion were taken into consideration. However, the filter effect related with the interface was not taken into account (see, for example, [15]).

## 2. MATHEMATICAL FORMULATION OF THE PROBLEM

From the qualitative pattern of the interaction between the solar wind and the partially ionized supersonic interstellar-gas flow described in the previous section there follows a complicated mathematical problem of the description of the motion of two interacting media. Its intricacy lies in the fact that the interaction of the plasma component of the interstellar medium with the solar wind can be described within the framework of the hydroaeromechanics equations, whereas for hydrogen atoms of different species we have  $Kn = l/L \geq 1$  and, therefore, their motion in the interaction region cannot be described by the continuum mechanics

equations (here,  $l$  is the free path of the H atoms in the resonance charge exchange process and the size of the heliosphere (Fig. 1) is taken as the scale length  $L$ ).

The first mathematical models of the phenomenon under consideration had a number of limitations; a detailed analysis can be found in [16, 17]. Thus, in [18] the continuum model was used to study the interaction between the solar wind and the interstellar gas flow for  $M_\infty \ll 1$  ( $M_\infty = V_\infty/a_\infty$ , where  $V_\infty$  is the interstellar gas velocity relative to the Sun and  $a_\infty$  is the speed of sound in the oncoming flow), though the first observations of the backscattered solar radiation already indicated the supersonic nature of the interstellar gas motion relative to the Sun. It was shown that the interstellar gas flow incident on the solar system is partially ionized [11] and is not hypersonic. These observation data were not in agreement with the assumptions made in [6]. The H atom effect on the flow under consideration was first investigated in a rather coarse approximation in [19], where only the effect of the atoms of species 4 was taken into account. The distribution of their number density was governed by the continuity equation with a ‘‘sink’’ term due to charge exchange, while for their temperature and velocity it was assumed that  $T_H = \text{const}$  and  $V_H = \text{const}$ , since the continuum mechanics equations cannot be applied at  $\text{Kn} = l/L \geq 1$ .

The best validated model was proposed in [20]; there the Euler equations with source terms governing the resonance charge exchange process were used for describing the plasma component. In the steady case these equations take the form:

$$\begin{aligned} \nabla \rho \mathbf{V} = 0, \quad (\mathbf{V} \nabla) \mathbf{V} + \frac{1}{\rho} \nabla p = \mathbf{F}_1[f_H(\mathbf{r}, \mathbf{w}), p, \mathbf{V}, \rho] \\ \nabla \left[ \rho \mathbf{V} \left( \varepsilon + \frac{p}{\rho} + \frac{V^2}{2} \right) \right] = F_2[f_H(\mathbf{r}, \mathbf{w}_H), p, \mathbf{V}, \rho], \quad p = (\gamma - 1) \rho \varepsilon \end{aligned} \quad (2.1)$$

Here,  $p$ ,  $\rho$ ,  $\varepsilon$ , and  $\mathbf{V}$  are the pressure, the density, the internal energy, and the velocity vector of the plasma component, respectively,  $\mathbf{F}_1$  and  $F_2$  are the momentum and energy sources for the plasma component due to resonance charge exchange,  $f_H$  is the hydrogen atom distribution function dependent on the radius-vector  $\mathbf{r}$  and the individual atom velocity  $\mathbf{w}_H$ , and  $\gamma = 5/3$  is the specific heat ratio for the fully ionized hydrogen plasma. The system of equations (2.1) is closed by adding the Boltzmann equation for the distribution function  $f_H$

$$\begin{aligned} \mathbf{w}_H \frac{\partial f_H(\mathbf{r}, \mathbf{w}_H)}{\partial \mathbf{r}} + \left[ \frac{\mathbf{F}_r + \mathbf{F}_g}{m_H} \right] \frac{\partial f_H(\mathbf{r}, \mathbf{w}_H)}{\partial \mathbf{w}_H} = f_p(\mathbf{r}, \mathbf{w}_H) \int |\mathbf{w}'_H - \\ \mathbf{w}_H| \sigma f_H(\mathbf{r}, \mathbf{w}'_H) d\mathbf{w}'_H - f_H(\mathbf{r}, \mathbf{w}_H) \int |\mathbf{w}_H - \mathbf{w}_p| \sigma f_p(\mathbf{r}, \mathbf{w}_p) d\mathbf{w}_p \end{aligned} \quad (2.2)$$

Equation (2.2) is linear, since the proton distribution function  $f_p(\mathbf{r}, \mathbf{w}_p)$  is assumed to be locally-Maxwellian with the gasdynamic values of the velocity vector  $\mathbf{V}(\mathbf{r})$ , temperature  $T(\mathbf{r})$ , and density  $\rho(\mathbf{r})$ ;  $\mathbf{w}_p$  is the individual proton velocity vector,  $\sigma(|\mathbf{w}_H - \mathbf{w}_p|)$  is the effective charge exchange cross-section, and  $\mathbf{F}_r$  and  $\mathbf{F}_g$  are the forces of solar radiative repulsion and gravitational attraction, respectively. The source terms on the right-hand sides of Eqs. (2.1) are calculated from the formulas

$$\begin{aligned} \mathbf{F}_1 = \frac{1}{n_p} \int d\mathbf{w}_H \int d\mathbf{w}_p \sigma |\mathbf{w}_H - \mathbf{w}_p| (\mathbf{w}_H - \mathbf{w}_p) f_H(\mathbf{r}, \mathbf{w}_H) f_p(\mathbf{r}, \mathbf{w}_p) \\ F_2 = m_H \int d\mathbf{w}_H \int d\mathbf{w}_p \sigma |\mathbf{w}_H - \mathbf{w}_p| \left( \frac{w_H^2}{2} - \frac{w_p^2}{2} \right) f_H(\mathbf{r}, \mathbf{w}_H) f_p(\mathbf{r}, \mathbf{w}_p) \\ n_H = \int d\mathbf{w}_H f_H(\mathbf{r}, \mathbf{w}_H), \quad n_p = \int d\mathbf{w}_p f_p(\mathbf{r}, \mathbf{w}_p) \end{aligned} \quad (2.3)$$

In order to apply the equations of ideal gasdynamics in the single-fluid approximation to the plasma component in form (2.1), it must be assumed that the electron and proton temperatures are the same; the

protons formed as a result of charge exchange immediately acquire the velocity and temperature of the plasma component (instantaneous “pickup” by the plasma or instantaneous “relaxation”); and the proton distribution function is locally Maxwellian.

For solving the integral Boltzmann equation (2.2) for the distribution function  $f_H$  and calculating the source terms in Eq. (2.1) from formulas (2.3), the improved Monte Carlo method with trajectory splitting was used. This method, developed for the problem under consideration in [21], ensures considerably greater accuracy than the direct Monte Carlo method.

The boundary conditions for the plasma component took the form of constant values of the velocity  $V_E$ , the electron (proton) number density  $n_E$ , and the Mach number  $M_E$  at the Earth’s orbit (subscript “E”) and the values of the same parameters in the local interstellar medium (subscript “∞”). Equations (2.1) were numerically solved by the Godunov method using the strong discontinuity fitting technique. Therefore, the Hugoniot relations must be fulfilled at the *TS* and *BS* shocks and the equal pressure and impermeability conditions (zero normal velocity) at the heliopause *HP* (Fig. 1). For hydrogen atoms it was assumed that in the interstellar medium their distribution function is Maxwellian with the number density  $n_{H\infty}$  and a temperature and velocity equal to the values of these parameters for the plasma component. Moreover, the ratio  $\mu = F_r/F_g$  of the solar radiative repulsion to the solar gravitation must be preassigned; for hydrogen atoms this ratio is near-unity. In the model considered in this section, the interstellar helium effect was not taken into account in view of its low abundance and small charge exchange cross-section.

For solving the axisymmetric problem thus formulated the global iteration method was used; the first stage consisted in solving a purely gasdynamic problem (with zero source terms in Eqs. (2.1)) of the supersonic parallel flow of a fully ionized gas (interstellar gas) past a spherically-symmetric supersonic source (solar wind). Then using the Monte Carlo method, the hydrogen atom trajectories were calculated in the gasdynamic flowfield, which made it possible to determine the source terms in the first approximation by means of formulas (2.3). The source terms calculated in this approximation were used for solving the gasdynamic part of the problem in the next iteration stage, in which the resonance charge exchange was taken into account. For calculating the H atom trajectories in the new gasdynamic flowfield, the Monte Carlo method was again used. The iteration procedure was performed until the next approximation gave negligibly small corrections (about 2%) to the previous approximation. In [20] the iteration process was terminated in the fourth stage.

Numerical calculations were carried out in a cylindrical coordinate system, while all the results presented below are given in a spherical reference frame with origin at the Sun and the angle  $\theta$  measured from the  $z$  axis directed toward the oncoming flow of the interstellar medium (the  $x$  axis is perpendicular to the  $z$  axis). In solving the kinetic part of the problem, in [20] the source terms were determined from formulas (2.3) without explicitly calculating the H atom distribution function. We note that in the problem formulated only the main process of resonance charge exchange was taken into account, though in certain flow regions the processes of ionization by solar radiation and electron impact, which can easily be incorporated within the framework of the model under consideration, can play an important role in interpreting the observation data. In this case, the right-hand side of the continuity equation is nonzero and the right-hand side of Eq. (2.2) includes the terms associated with these processes [21].

### 3. MAIN RESULTS FOR MODEL [20]

For obtaining quantitative results on the basis of the model presented in the previous section, the following values of the parameters at the Earth’s orbit and in the interstellar medium were used:

$$\begin{aligned} n_E &= 7 \text{ cm}^{-3}, & V_E &= 450 \text{ km} \cdot \text{s}^{-1}, & M_E &= 10, & \mu &= 0.75 \\ n_{p\infty} &= 0.07 \text{ cm}^{-3}, & V_\infty &= 25 \text{ km} \cdot \text{s}^{-1}, & M_\infty &= 2, & n_{H\infty} &= 0.14 \text{ cm}^{-3} \end{aligned} \quad (3.1)$$

*Results for the plasma component of the flow.* In Fig. 2 the positions of the strong discontinuity surfaces are presented. On the coordinate axes the distances are measured in astronomical units (a.u.). For the sake

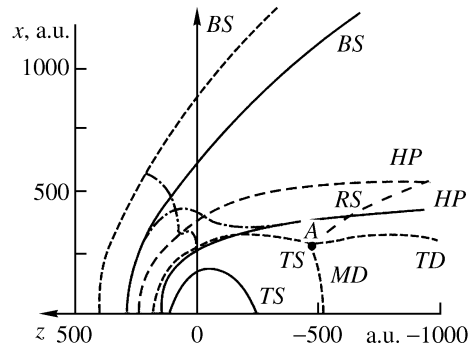


Fig. 2. *BS*, *TS*, and *HP* positions calculated within the framework of model [20]; the broken and chain curves represent the strong discontinuity surfaces and sonic lines, respectively, calculated in the absence of charge exchange ( $n_{H\infty} = 0$ )

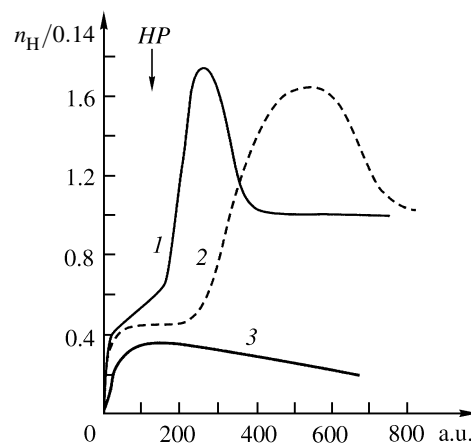


Fig. 3. Distribution of the sum of the concentrations  $n_H$  of the hydrogen atoms of species 3 and 4 calculated in accordance with model [20]. The hydrogen barrier is represented in the form of a nonmonotonic distribution. Curves 1 and 3 are the profiles along the axis of symmetry in the nose and tail regions and curve 2 is the profile in a direction perpendicular to the axis of symmetry

of comparison, the calculated results for the purely gasdynamic problem ( $n_{H\infty} = 0$ ) are also presented. The comparison shows that the charge exchange process results in a considerable decrease in the heliocentric stand-off distances of the shock waves and the heliopause and the collapse of the complicated flow structure in the tail region consisting of a Mach disk (*MD*), a tangential discontinuity (*TD*), and a reflected shock (*RS*). This implies the absence of a triple point *A*, at which the supersonic flow is deflected, and the formation of a smooth closed surface of the *TS* shock with a subsonic flow throughout the entire inner interface (region 2 in Fig. 1). For the parameter values (3.1), the inner shock is located at a distance  $r_{TS} \sim 80$  a.u. and the heliosphere boundary (heliopause) at a distance  $r_{HP} \sim 150$  a.u. from the Sun along the  $z$  axis (in the direction of the oncoming flow).

The results for the model considered also indicate that resonance charge exchange leads to an approximately 10% decrease in the solar wind velocity ahead of the *TS* shock and to its heating. However, the assumption concerning the instantaneous pickup (relaxation) of the protons formed as a result of charge exchange leads to an overestimated value of the temperature (see Section 4). The calculated results indicate the important role of the  $H_{SW}$  atoms (Fig. 1) related with the process of their charge exchange with interstellar protons. In particular, this consists in a reduction of the Mach number in region 4 and the appearance of a velocity component perpendicular to the axis of symmetry  $z$  in this region.

*Results for hydrogen atoms.* One of the main results obtained using model [20] is the prediction of the formation of three species of H atoms as a result of charge exchange between the primary atoms of the in-

terstellar medium (species 4) and the solar wind protons (species 1 and 2) and their own protons (species 3). The Monte Carlo method used here makes it possible to take account of multiple charge exchanges and to calculate the parameters of each species. The parameters of atoms of different species can be quite different, since the new atoms acquire the parameters of the protons in the regions where they were born.

In Fig. 3 the sum of the number densities of the primary and secondary H atoms (species 4 and 3, respectively) is plotted against the heliocentric distance. The parameters of precisely these H atoms penetrating from the interstellar medium into the solar system have been measured onboard spacecraft from the backscattered solar Lyman- $\alpha$  radiation [8, 9, 15]. Their number density is a nonmonotonic function of the heliocentric distance with a maximum ahead of the heliopause. This unexpected effect obtained in the calculations was named the “hydrogen barrier” and later detected onboard the *Hubble Space Telescope* (Section 5). The physical significance of hydrogen barrier formation can easily be explained in terms of local interstellar medium proton deceleration near the heliopause. As a result of charge exchange with the decelerating protons, decelerating hydrogen atoms of species 3 are formed, which leads, due to the fact that they obey the continuity equation, to an increase in their density. The hydrogen barrier is most clearly expressed near the stagnation point on the heliopause; at the same time, it is absent from the tail region. It is also obvious that the number of primary H atoms (of species 4) decreases monotonically as the Sun is approached, in view of their continuous depletion by charge exchange (and photoionization).

In conclusion, we note that within the framework of the model considered the calculated H atom temperature distributions [22] are different in the radial and transverse directions. This is a demonstration of the fact that the distribution function  $f_H$  is not equilibrium, so that we can speak only of the “effective” temperature as a measure of the chaotic motion of the atoms. Below, we will consider the detailed characteristics of the neutral atoms of species 2 born in the inner interface.

#### 4. DEVELOPMENT OF THE MODEL PROPOSED IN [20]

The new experimental data obtained onboard the spacecraft listed above make it necessary to refine and develop model [20]. The main difficulty in constructing a complete model consists in the multicomponent nature of both the local interstellar medium and the solar wind. The effect of certain components, such as, for example, atoms of helium, oxygen, nitrogen, and others, is negligible in view of their low cosmic abundance as compared with that of hydrogen atoms (see Section 5). The effect of the galactic cosmic rays is also small as compared with that of H-atom resonance charge exchange [23]. The interplanetary magnetic field effect can be neglected in the supersonic region of the solar wind (region 1) in view of the inequality  $M_A = \sqrt{4\pi\rho} V_E / B \gg 1$ , where  $M_A$  is the alfvénic Mach number, though its role in region 2 is still poorly understood. A magnetic field may be present in the interstellar medium. However, its value and direction in the vicinity of the solar system are practically unknown. Nevertheless, bearing in mind the interpretation of the experimental data, the MHD nature of the solar wind/interstellar gas interaction must be studied with the interstellar magnetic field as an unknown parameter. This problem is generally three-dimensional.

Below, we will consider the physical phenomena that complement — to some degree or another — the model proposed in [20]. Sometimes, taking account of certain processes which at first glance have little effect on the results provided by the model can play an important role in interpreting the experimental data. Thus, taking the alpha-particles of the solar wind and the ionized helium in the interstellar medium into account [24] leads to a slight variation (of about 2%) in the TS shock position, which can amount to about 2 a.u. Nevertheless, this value may be important for interpreting the measurements onboard the spacecraft *Voyager 1* and *2* which are moving away from the Sun at a velocity of about 3.5 a.u./yr.

*Effect of the anomalous component of cosmic rays.* The anomalous and galactic components of cosmic rays, whose spectra are appreciably different, can be considered as high-energy (often relativistic) populations with a negligible mass density, as compared with that of the plasma, but a considerable (non-negligible) energy density. The origin of the galactic cosmic ray acceleration lies outside the solar system, while the origin of the anomalous component acceleration is recognized to be the TS shock. On the hydrodynamic level, the cosmic ray effect on the flow of the carrier plasma component is described by the cosmic ray

pressure gradient  $\nabla p_{cr}$  and the energy transport  $\mathbf{V}\nabla p_{cr}$  from the carrier phase to the cosmic rays. For the galactic cosmic rays these terms in Eq. (2.1) are small as compared with the source terms [23]; this makes it possible to neglect their effect on the flow. Generally, the cosmic ray pressure is determined by the formula

$$p_{cr} = \frac{4\pi}{3} \int_0^{\infty} f_{cr}(\mathbf{r}, |\mathbf{p}|, t) |\mathbf{p}|^4 d|\mathbf{p}|$$

where  $f_{cr}(\mathbf{r}, |\mathbf{p}|, t)$  is the isotropic function of the cosmic ray distribution and  $|\mathbf{p}|$  is the magnitude of the particle momentum. Integration of the equation for  $f_{cr}$  (the form of this equation can be found, for example, in [25]) over the momentum magnitude leads to the following equation for  $p_{cr}$

$$\frac{\partial p_{cr}}{\partial t} = \nabla[\kappa \nabla p_{cr} - \gamma_{cr}(\mathbf{V} + \mathbf{V}_d)p_{cr}] + (\gamma_{cr} - 1)\mathbf{V}\nabla p_{cr} + Q \quad (4.1)$$

Here,  $\kappa$  is the cosmic ray diffusivity determining the spatial diffusion,  $\mathbf{V}$  is the mean velocity of the plasma,  $\mathbf{V}_d$  is the drift velocity in the heliospheric or interstellar magnetic field averaged over the distribution function  $f_{cr}$ ,  $\gamma_{cr}$  is the polytropic exponent of cosmic rays, and  $Q$  is the source term governing the effect of the pickup protons on the anomalous component of the cosmic rays (energy influx and efflux due to the birth and decay of protons as a result of forward and backward charge exchange, photoionization, and electron impact ionization [25]). In [25] the following expression for the source term was used:

$$Q = -\alpha p \nabla \mathbf{V} \quad (4.2)$$

where  $\alpha$  is a coefficient determining the rate of injection of charged particles subjected to acceleration up to the anomalous component of cosmic rays in the  $TS$  shock, and  $p$  is the plasma component pressure determined from the system of equations (2.1). Usually, the coefficient  $\alpha$  is a free parameter, whose order of magnitude is determined by the plasma properties (for galactic rays this coefficient is taken to be zero, since the origin of their acceleration lies outside the heliosphere).

The dynamic effect of the anomalous component on the heliospheric interface structure was studied in [26]. The system of equations (2.1) and (2.2), which included the pressure gradient  $p_{cr}$ , was closed by Eqs. (4.1) and (4.2). The effects associated with the influence of the cosmic ray diffusivity were studied at a constant injection coefficient, since at present the diffusivity coefficients in the outer heliosphere and, in particular, in the interface are poorly known. The anomalous component effect on the solar wind flow in the vicinity of the heliospheric  $TS$  shock leads to smooth deceleration of the solar wind in the so-called precursor followed by the shock [26]. The intensity of the shock decreases and, as a result, it is located at a greater heliocentric distance than when the anomalous component effect is disregarded [20]. Both the shock intensity and the value of its displacement depend on the diffusivity coefficient. A decrease in the shock intensity is accompanied by a decrease in the temperature of the inner interface, which is important for interpreting the measurements of the fluxes of H atoms of species 2 at 1 a.u. which the United States plans to make onboard the IBEX<sup>1</sup> spacecraft in 2008. The maximum shock displacement (about 4 a.u.) is realized for intermediate values of the diffusivity. The heliospheric shock precursor is most clearly expressed for low diffusivity values and vanishes at large values. This can be attributed to the fact that in the former case the diffusion scale length is much smaller than the distance to  $TS$ , the cosmic ray pressure behind  $TS$  being comparable with the static pressure of the plasma. In the latter case the cosmic ray pressure is negligible as compared with the static pressure of the plasma, so that the effect of the anomalous component of the cosmic rays on the results [20] can be neglected.

In interpreting the anomalous component measurements, it is important to note that, due to the difference in the amounts of energy injected into it in the forward (relative to the oncoming interstellar medium flow) and tail regions of the heliospheric shock, there is a clearly expressed angular energy asymmetry. This is due to the fact that the static pressure of the plasma is lower in the tail than in the forward region.

---

<sup>1</sup>Interstellar Boundary Explorer.

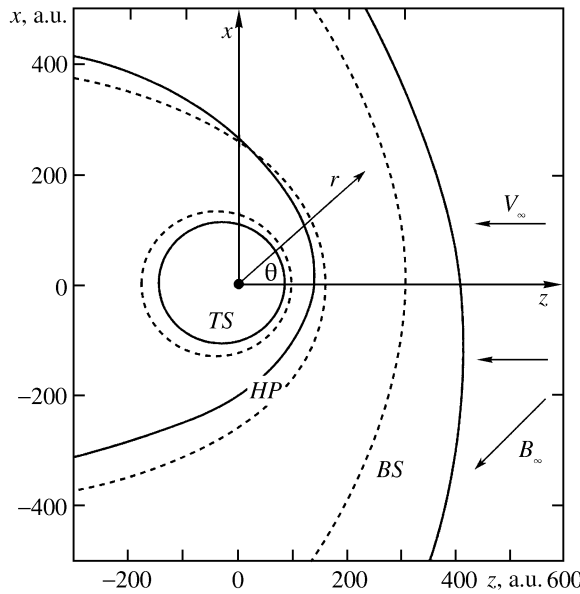


Fig. 4. Positions of the strong discontinuity surfaces *TS*, *HP*, and *BS* with account for the interstellar magnetic field [28]. The broken curves denote the results calculated within the framework of model [20] ( $\mathbf{B}_\infty = 0$ )

*Interstellar magnetic field effect.* The effect of the interstellar magnetic field on the flows of the plasma component and hydrogen atoms was first considered within the framework of model [20] in [27]. To retain axial symmetry, in [27] the interstellar magnetic field vector  $\mathbf{B}_\infty$  was assumed to be parallel to the velocity vector  $\mathbf{V}_\infty$ .

Recently, in [28], the interstellar magnetic field effect on the heliospheric interface structure was studied for the general three-dimensional case. In this case, the equation of motion for the plasma component (second equation (2.1)) included the ponderomotive force  $1/4\pi(\nabla \times \mathbf{B}) \times \mathbf{B}$  and the system of equations (2.1)–(2.3) was closed by the equation for the magnetic field induction  $\mathbf{B}$  in the high magnetic Reynolds number approximation ( $\text{Re}_m \gg 1$ )

$$\nabla \times (\mathbf{V} \times \mathbf{B}) = 0$$

As the boundary conditions the following parameters in the undisturbed interstellar medium and the solar wind at the Earth’s orbit were used:

$$\begin{aligned} V_\infty = 26.4 \text{ km/s}, \quad M_\infty = 2, \quad n_{\text{H}\infty} = 0.18 \text{ cm}^{-3}, \quad n_{p\infty} = 0.06 \text{ cm}^{-3}, \\ B_\infty = 2.5 \text{ }\mu\text{Gs}, \quad V_E = 432 \text{ km/s}, \quad M_E = 10, \quad n_E = 7.39 \text{ cm}^{-3} \end{aligned}$$

It was assumed that the interstellar magnetic field makes an angle  $\theta = 45^\circ$  with the oncoming flow. For the parameter values listed above we have  $M_{A\infty} = V_\infty/a_{A\infty} = 1.18$  and  $M_{fs} = V_\infty/a_{+\infty} = 1.01$ , where  $a_{A\infty}$  is the alfvénic speed of sound and  $a_{+\infty}$  is the speed of the fast magnetosonic wave in the interstellar medium.

In Fig. 4 we have plotted the calculated positions of the strong discontinuity surfaces (the *TS* and *BS* shocks and the tangential discontinuity, or heliopause, *HP*) in the *xz* plane determined by the vectors  $\mathbf{V}_\infty$  and  $\mathbf{B}_\infty$ . As in [20], the *z* axis is directed opposite to the vector  $\mathbf{V}_\infty$ , while the *x* axis is perpendicular to this vector. Figure 4 clearly indicates the flow asymmetry about the *z* axis. Taking the magnetic field into account causes the *TS* shock to approach and the *BS* shock to recede from the Sun. The heliocentric stand-off distance of *HP* depends on the magnetic pressure to magnetic tension ratio. In the regions where the magnetic tension is greater than the magnetic pressure, the heliopause recedes from the Sun [27]. Obviously, the maximum and minimum of the interstellar magnetic field pressure change places in accordance with the directions  $\theta = -45^\circ$  and  $45^\circ$ . The *TS* and *HP* surfaces move closer to the Sun by 10 and 20 a.u., respectively. As a result of the heliopause asymmetry, the interstellar plasma density is greater in the upper ( $x > 0$ ) than

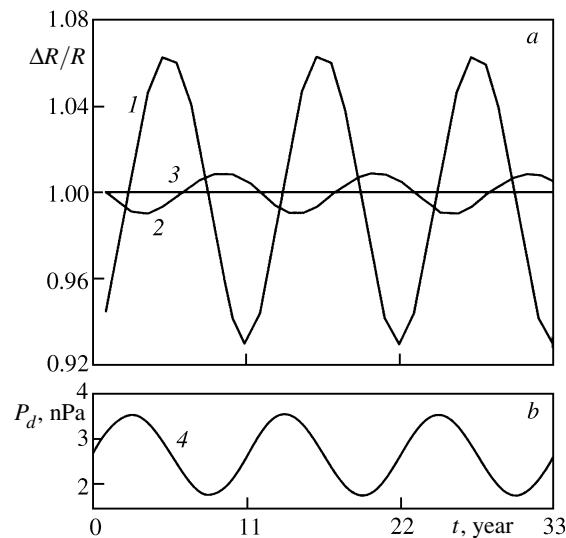


Fig. 5. Time variation of the strong discontinuity surface position in the nose region of the heliospheric interface as a function of the 11-year solar activity cycle. Curves 1, 2, and 3 relate to the variation of *TS*, *HP*, and *BS* position and curve 4 to the variation of the ram pressure at the Earth's orbit

in the lower ( $x < 0$ ) half-plane. Calculations showed that the stagnation point on the heliopause is about  $10^\circ$  above the  $z$  axis. In the vicinity of this point the density of the interstellar medium plasma component reaches a maximum, while its velocity vector has a considerable  $x$ -component  $V_x$ . Since the parameters of the H atoms of species 3 are consistent with those of the plasma in the outer interface region, they also have a velocity component along the  $x$  axis. As might be expected, in this case the maximum intensity of the hydrogen barrier is reached precisely near the stagnation point (Fig. 3).

The vector  $\mathbf{V}_H$  of the mean velocity of the hydrogen atoms was calculated as the moment of the distribution function  $f_H$ . Its component along the  $x$  axis is nonzero even at small heliocentric distances. In the calculations the angle between the mean velocity of the hydrogen atoms within the heliopause and the direction of the interstellar medium motion was 3 to  $5^\circ$  [28]. The same deviation of the hydrogen atom motion direction was recently detected from measurements of the backscattered solar Lyman- $\alpha$  radiation made onboard the spacecraft SOHO<sup>2</sup> [29], which can be attributed to the interstellar magnetic field effect.

*Effect of the 11-year solar activity cycle.* The solar wind parameters have already been measured onboard spacecraft over about four solar cycles (about 45 years). The measurements showed [30] that the solar wind ram pressure changes by a factor of about two on transition from maximum to minimum solar activity. In certain studies, the effect of the time variation of the solar wind ram pressure on the heliospheric interface was investigated. However, in [31] the effect of interstellar H atoms was not taken into account, while in [32] they were accounted for within the framework of a simplified (multifluid) model which, as shown above, is not justified for neutral atoms.

In [33] the self-consistent time-dependent problem of the interaction between the two-component (plasma component and H atoms) interstellar medium and the solar wind was solved in the axisymmetric approximation. For studying the solar cycle effect a periodic solution of the time-dependent equations (2.1) for the plasma, together with the time-dependent kinetic equation (2.2) for the H atoms, was obtained. For solving Eq. (2.2) a time-dependent Monte Carlo method was developed. Periodic values of the parameters at the Earth's orbit were taken as the boundary conditions. In particular, in [34] the results for an "ideal" solar cycle, in which the solar wind ram pressure varies sinusoidally with an oscillation amplitude equal to 2 and a period of 11 years, are presented.

<sup>2</sup>Solar and Heliospheric Observatory

Figure 5 shows the 11 year-periodic variations of the strong discontinuity surface (*TS*, *HP*, and *BC*, see Fig. 1) positions in the nose part of the heliopause along the axis of symmetry. The heliospheric shock *TS*, the heliopause *HP*, and the bow shock *BS* oscillation amplitudes are equal to about 7.5 a.u., about 2 a.u., and less than 0.7 a.u., respectively. As we move from the nose to the tail region, the *TS* oscillation amplitude increases and can amount to 25 a.u. [34]. In the nose and tail regions, the oscillations are almost in antiphase. The *TS* response to ram pressure variation at the Earth's orbit takes place with a delay of about two years (Fig. 5). The calculated results indicate that the plasma parameters also perform oscillations with an 11-year period throughout the entire interface region.

In the solar wind, the oscillation wavelength is greater than the distance to the *TS* shock and the heliopause *HP* in the nose part of the heliosphere. The situation is essentially different in the outer interface region between the heliopause and the bow shock. The heliopause motion acts on the interstellar medium in the same way as a piston in motion in a tube filled with gas and leads to the formation of a sequence of shock and rarefaction waves. The amplitudes of these waves decrease as they travel away from the Sun, which is due to the divergent nature of the motion. The decrease in amplitude is also due to the interaction between the shock and rarefaction waves. In the nose region the characteristic wavelength is about 40 a.u.

It is interesting to note that the values of the solar-cycle-averaged heliocentric stand-off distances of the shocks and the heliopause, as well as the plasma parameter distributions, are similar to those obtained within the framework of the stationary model [20] with solar-cycle-averaged boundary conditions. There is a clearly expressed 11-year periodicity in the distributions of the interstellar H atom density. In the outer regions of the solar wind, in particular, in the vicinity of the *TS* shock, the fluctuations of the densities of the primary and secondary interstellar H atoms (of species 4 and 3) lie within  $\pm 5\%$  of their mean values. The same fluctuation level is characteristic of the H atoms of species 2. The fluctuations of the density of the H atoms of species 1 amount to  $\pm 30\%$  of their mean values.

The calculations also showed that the fluctuations of the mean bulk velocity and the "effective" temperature of H atoms of species 3 and 4 (averaged over the nonequilibrium distribution function) are negligible. As for the mean bulk velocity and kinetic temperature of the atoms of species 2, they vary by 10 to 12% during a solar cycle. These fluctuations can be attributed to the fact that the largest number of atoms of this species is born in the vicinity of the heliopause, and the long-wave nature of the fluctuations characteristic of the plasma in this region is reflected in the distribution of the H atoms of species 2.

*Heliosphere extent in the tail region.* The main purpose of modeling the tail region of the heliospheric interface is to find the answers to two fundamental questions: (1) where is the heliopause boundary and (2) what is the extent of the influence of the solar wind on the surrounding interstellar medium? To answer the first question we must first define the heliosphere boundary. For this boundary, it would be natural to take the heliopause separating the solar-wind and interstellar-medium plasmas. However, such a definition would be incorrect, since the heliopause is an unclosed surface and the tail part of the heliosphere could extend to infinity in the absence of mixing of the solar wind plasma and the interstellar medium flow at large heliocentric distances. In order to solve this problem and to answer the second question, in [35] the structure of the tail region of the heliospheric interface was studied in detail at large (up to 30,000 a.u.) heliocentric distances (in [20] the heliospheric tail region was calculated only to distances of about 700 a.u., see Fig. 2).

The results of the calculations performed in [35] are presented in Fig. 6. Immediately after crossing the heliospheric shock *TS* the solar wind plasma acquires a subsonic velocity of about 100 km/s and a temperature of about  $1.5 \cdot 10^6$  K. Then the solar wind velocity continues to decrease due to "mass-loading" by new protons born as a result of charge exchange and gradually approaches a velocity typical of the undisturbed interstellar medium flow ( $V_\infty \sim 25$  km/s). Since the interstellar atom temperature is much lower than the proton temperature behind the heliospheric shock, charge exchange leads to effective cooling of the solar wind in the tail region. As a result of this cooling, the solar wind Mach number increases, so that at a distance of about 4000 a.u. it again becomes supersonic. With further increase in the heliocentric distance, the plasma and H atom parameters approach their values in the local interstellar medium ( $M_\infty = 2$ ). The calculations showed that at distances of about 40 to 50,000 a.u. the solar wind parameters are almost

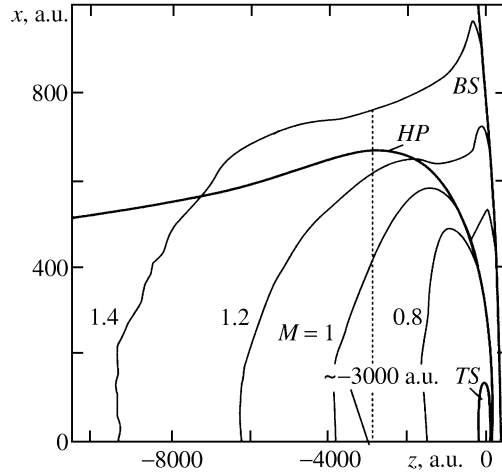


Fig. 6. Mach number contours for the solar-wind and interstellar-medium plasmas in the tail region of the heliospheric interface

indistinguishable from those of the undisturbed interstellar medium. These distances can be regarded as the heliosphere boundary in the tail region. It is also interesting to note that the jumps in density and tangential velocity at the tangential discontinuity *HP* almost vanish at considerably smaller heliocentric distances (of about 3000 a.u.).

*Effect of nonequilibrium of the pickup protons and solar protons in the solar wind.* In model [20] the single-fluid approximation is used for the charged component. However, measurements of the pickup proton distribution function onboard the *Ulysses* and ACE spacecraft showed that the pickup proton distribution function is non-Maxwellian, though isotropic. These data pointed to the absence of thermodynamic equilibrium between the pickup and solar-origin protons, although their mean velocities are equal.

In the improved model of the solar wind/interstellar medium interaction developed in [36], the pickup protons are considered as a separate component with thermodynamic parameters different from those of the solar wind. Since in the solar-wind-fitted reference frame the pickup proton distribution function is isotropic, the following angle-averaged distribution function can be introduced:

$$f_{pui}(\mathbf{r}, \mathbf{w}) = \frac{1}{4\pi} \int \int f_{pui}^*(\mathbf{r}, \mathbf{v}) \sin \theta d\theta d\varphi$$

Here,  $\mathbf{v}$  is the individual velocity of a pickup proton,  $\mathbf{w} = \mathbf{v} - \mathbf{V}$  is the pickup proton velocity in the solar-wind-fitted reference frame ( $\mathbf{V}$  is the solar wind velocity in the heliocentric coordinate system),  $w$ ,  $\theta$ , and  $\varphi$  are the coordinates of the vector  $\mathbf{w}$  in the spherical coordinate system, and  $f_{pui}^*(\mathbf{r}, \mathbf{v})$  is the pickup proton distribution function. The kinetic equation for  $f_{pui}(\mathbf{r}, \mathbf{w})$  can be written in the form:

$$\frac{\partial f_{pui}}{\partial t} + \mathbf{v} \frac{\partial f_{pui}}{\partial \mathbf{r}} = \frac{1}{w^2} \frac{\partial}{\partial w} \left( w^2 D \frac{\partial f_{pui}}{\partial w} \right) + \frac{w}{3} \frac{\partial f_{pui}}{\partial w} \nabla \mathbf{V} + S(\mathbf{r}, w) \quad (4.3)$$

Here,  $D(\mathbf{r}, w)$  is the diffusivity in velocity space, while the source of the pickup protons  $S(\mathbf{r}, w)$  reflects their birth and loss due to charge exchange, photoionization, and the electron impact ionization of H atoms.

In [36] the kinetic equation (4.3) was solved together with the Euler equations (2.1) written for the sum of all the charged components and the kinetic equation (2.2) for the interstellar hydrogen atoms. The use of Eq. (2.1) for the sum of the charged components is justified by the fact that all the components (solar protons and electrons, as well as pickup protons) move at the same velocity and for all the components the distribution functions are isotropic. In this case, the pressure  $p$  is equal to the sum of partial pressures, while the effective pressure of the pickup protons is determined in terms of the distribution function  $f_{pui}$  as follows:

$$p = p_e + p_p + p_{pui}, \quad p_{pui} = \frac{4\pi}{3} \int m_p w^4 f_{pui}(\mathbf{r}, w) dw \quad (4.4)$$

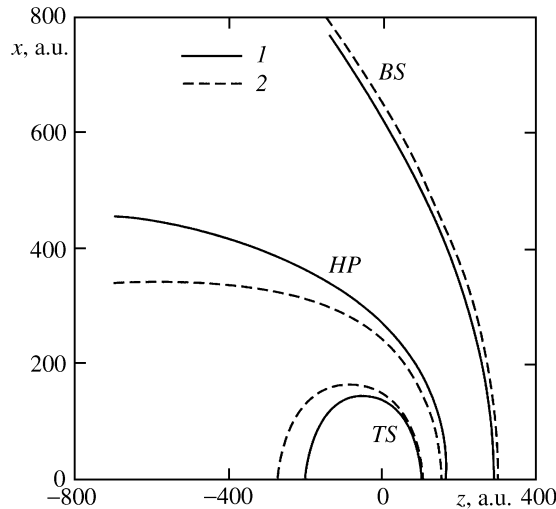


Fig. 7. Strong discontinuity surfaces calculated with account for pickup proton nonequilibrium [36] (curves 1) and in accordance with model [20] (curves 2)

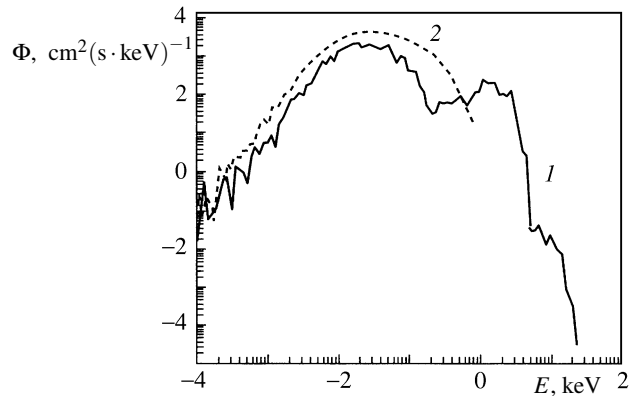


Fig. 8. Fluxes of H atoms of species 2 at 1 a.u. (curve 2). For the sake of comparison, curve 1 represents the fluxes calculated within the framework of model [20]

In [36] the system of equations (2.1), (2.2), and (4.3) was solved using the total pressure (4.4) under the assumption of equality of the electron and proton temperatures ( $T_e = T_p$ ). From the condition of conservation of the adiabatic invariant on *TS*, which is a quasi-normal shock, there follows the boundary condition on that shock

$$f_{pui,2}(\mathbf{r}, w) = \beta^{-1/2} f_{pui,1}(r, w/\sqrt{\beta}), \quad \beta = \rho_2/\rho_1$$

where  $\beta$  is the compression ratio across the shock. A self-consistent solution of the problem formulated was obtained in [36] for the case  $D = 0$  corresponding to a quiescent solar wind in which the magnetic field fluctuation level is low.

The thermodynamic nonequilibrium of the pickup and solar protons leads to a thinning of the inner interface region (Fig. 7), which is attributable to a decrease in the total pressure of the charged component determined by Eq. (4.4). As compared with the calculations performed in accordance with model [20], the *TS* shock is 5 a.u. farther from the Sun in the direction of the oncoming flow, whereas the heliopause *HP* is 12 a.u. closer. In the tail region the heliocentric distance of *TS* increases by 70 a.u. This refinement of the physical properties of the inner interface in connection with nonequilibrium is important for planning experiments to measure the fluxes of energetic H atoms from this region (H atoms of species 2) at 1 a.u. onboard the IBEX satellite. In Fig. 8 the calculated results for these fluxes at 1 a.u. obtained within the framework of model [36] are presented. The model with nonequilibrium taken into account predicts smaller

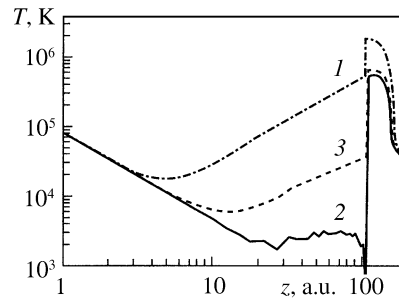


Fig. 9. Solar wind proton temperature vs the heliocentric distance: 1 corresponds to model [20], 2 to [36], and 3 to the calculations for the case in which 5% of the thermal energy is transferred from the pickup ions to the proton component

fluxes for particles with energies less than 1 keV and larger fluxes for particles with energies greater than 1 keV, as compared with the model [20]. Particles with energies of 1 keV and higher are chiefly formed during charge exchange between the interstellar hydrogen atoms and pickup protons. As for the particles with lower energies, these are formed during charge exchange with solar protons.

In accordance with model [20], the strong increase in temperature at large heliocentric distances (curve 1 in Fig. 9) is due to the assumption of instantaneous relaxation of the pickup protons in the solar wind. The measurements of the solar proton temperature onboard the *Voyager 2* spacecraft indicate that such considerable heating of the solar wind does not occur. The solar proton temperature obtained within the framework of model [36] (curve 3 in Fig. 9) decreases adiabatically up to a distance of about 20 a.u., then decreases more slowly than adiabatically, and starts to increase slowly at distances greater than 30 a.u. This behavior of the solar wind temperature is associated with the energy of the electrons born in the photoionization process (in the model it is assumed that  $T_e = T_p$ ). The temperature obtained from model [36] turns out to be lower than the solar wind temperature measured onboard *Voyager 2*. This means that the energy supplied to the solar wind is greater than the photoelectron energy. For this reason, in [36] calculations, in which it was assumed that there is heliocentric-distance-independent exchange of thermal energy (about 5%) between the solar-wind particles and the pickup protons, whose temperature is much higher than that of the solar protons, were carried out. The temperature distributions thus calculated (curve 2 in Fig. 9) are in good agreement with the measurements made onboard *Voyager 2*.

## 5. MODEL PREDICTIONS VERSUS EXPERIMENTS

In order to predict experimental data and interpret the results of measurements made onboard spacecraft exploring the outer regions of the solar system, a validated theoretical model must be available. In considering the problem of the solar wind/interstellar medium interaction in this paper emphasis is placed on the kinetic-gasdynamic model [20], since the other available models, which were developed considerably later (see, for example, [37]) and provide, as shown in [22, 28], incorrect results, are based on the multifluid approximation, including the description of neutral H atoms of all species. In the problem under consideration, the inapplicability of continuum mechanics for describing the neutral H atom motion was explicitly demonstrated by the results of [39], where the distribution function was calculated using the Monte Carlo method [21]. These calculations showed that in the heliopause the distribution functions of H atoms of all species are essentially non-Maxwellian, which is only natural for  $Kn \sim 1$ .

*Experimental discovery of the hydrogen barrier.* Model [20] made it possible to establish the hydrogen barrier phenomenon, that is, a nonmonotonic distribution of interstellar hydrogen atoms of species 3 with a peak near the heliopause (Fig. 3). It is interesting to note that this phenomenon was first established in [40], in solving the non-self-consistent problem (the first iteration stage of the Monte Carlo method using the gasdynamic flowfields without source terms). The first communication on the experimental detection of the hydrogen barrier [41] based on the interpretation of the observed absorption spectra of the hydrogen

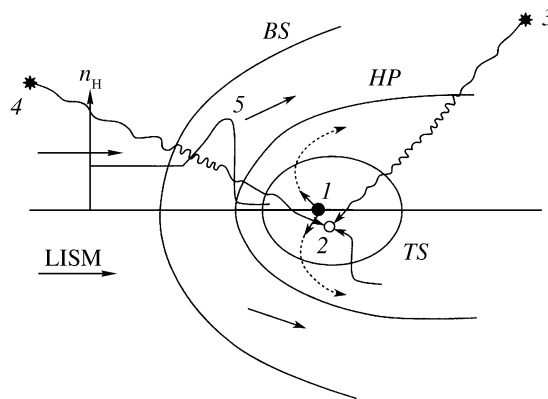


Fig. 10. Schematics of an experiment on the absorption of the Lyman- $\alpha$  emission of near stars; 1 denotes the Sun, 2 — the instrument receiving the star emission, 3 — Sirius, 4 —  $\alpha$  Cen, and 5 — the hydrogen barrier; LISM is the local interstellar medium flux

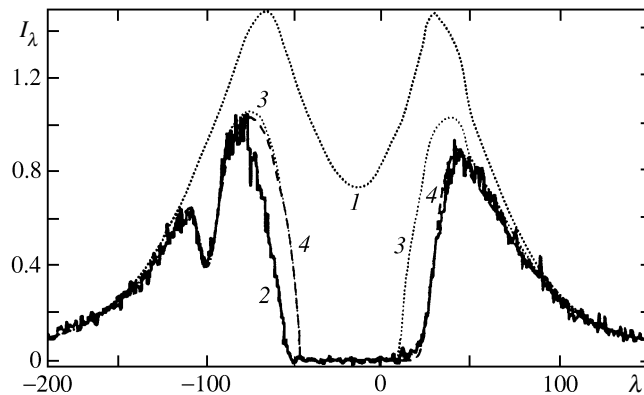


Fig. 11. Lyman- $\alpha$  absorption spectrum from  $\alpha$  Centauri: 1 —  $\alpha$  Centauri emission spectrum; 2 — absorption spectrum measured by the GHRIS instrument onboard the Hubble Space Telescope; 3 — the spectrum after absorption by hydrogen atoms in the local interstellar medium; and 4 — the spectrum obtained with account for absorption in the hydrogen barrier

Lyman- $\alpha$  emission from the  $\alpha$  Centauri star using the GHRIS<sup>3</sup> instrument onboard the American HST<sup>4</sup> spacecraft was made in [42]. A schematic diagram of these observations is shown in Fig. 10. If the emission spectrum of a star (say,  $\alpha$  Cen) is known, then the instrument at point 2 in Fig. 10 (point 1 coincides with the Sun) receives spectra corresponding to the absorption of this emission along the line of sight. This absorption occurs chiefly in the interstellar gas, while the right limb of the spectra received by the instrument (Fig. 11) could be attributed by the authors of [41] only to absorption in the heliospheric hydrogen barrier (4 in Fig. 10), since the right limb corresponds to the Doppler redshift (the motion of the interstellar H atoms is directed toward the instrument). The maximum intensity of the hydrogen barrier is associated with the polar angle  $\theta = 0$  (Fig. 3). For this reason, it is star observations at small polar angles that provide most information. The absorption spectra from the star 36Oph ( $\theta = 12^\circ$ ) observed using the STIS<sup>5</sup> instrument onboard the same HST spacecraft [43] supported the data of the observations in the direction of  $\alpha$  Cen ( $\theta = 52^\circ$ ). The absorption spectrum obtained by the GHRIS instrument onboard HST in the direction of Sirius (Fig. 12), when the line of sight makes an angle  $\theta = 139^\circ$ , was analyzed in [44]. The authors of [44] were able to provide an explanation of the spectrum obtained only by invoking absorption on hydrogen atoms of species 2, since at large polar angles the hydrogen barrier has a very low intensity.

<sup>3</sup>Goddard High Resolution Spectrometer.

<sup>4</sup>Hubble Space Telescope.

<sup>5</sup>Space Telescope Imaging Spectrograph.

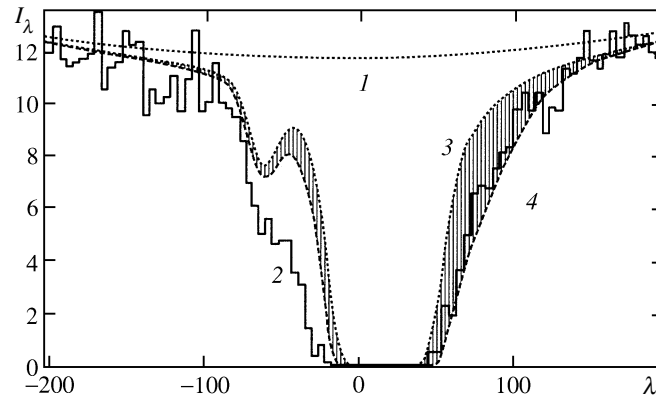


Fig. 12. Lyman- $\alpha$  absorption spectrum from Sirius; notation same as in Fig. 11

It is interesting to note that the left limb of the absorption spectra (Figs. 11 and 12) can be attributed to absorption in the hydrogen barriers of the stars observed [43, 44], which, in turn, indicates the presence of stellar winds from these stars.

*Experimental confirmation of the interface.* The notion of the interface, as the region between the *BS* and *TS* shocks, first introduced in [6] and developed in the best validated version in [20], was completely ignored by experimentalists up to 1985. However, for more than 20 years the experimental data obtained onboard the spacecraft exploring the outer regions of the solar system have had to be interpreted in the light of this notion. The question arises: what experimental data are there to confirm the existence of the interface?

Even on the basis of the first measurements of H and He atom concentrations from the backscattered solar radiation on 1216 and 584 Å wavelengths [8–10] it could be inferred that in the heliosphere the ratio  $n_{\text{He}}/n_{\text{H}} \sim 0.2$ , which is twice as large as its value in outer space (about 0.1). This can easily be explained by the presence of the heliospheric interface, where the interstellar H atoms are “filtered out” due to their large charge exchange cross section as compared with that of the He atoms, which penetrate into the heliosphere from the interstellar medium without changing their parameters. The experimental discovery of the hydrogen barrier also indicated the presence of the interface, since the barrier is a physical consequence of the heliopause separating the interstellar medium plasma component and the solar wind. However, the most weighty evidence of the presence of the interface was obtained onboard the SOHO and *Ulysses* spacecraft.

Ground-based measurements of the H atom and proton concentrations in the local interstellar medium usually led to their being estimated to within a factor of 2 and an order of magnitude, respectively. Since the proton concentration in the local interstellar medium largely determines the interface filter efficiency, in [24] a parametric investigation of the heliospheric interface structure was carried out within the framework of model [20] for proton and H atom concentrations ranging from 0.03 to 0.1  $\text{cm}^{-3}$  for  $n_{p\infty}$  and from 0.16 to 0.2  $\text{cm}^{-3}$  for  $n_{\text{H}\infty}$ , which approximately corresponds to the observation data [11]. For each  $(n_{\text{H}\infty}, n_{p\infty})$  pair the H atom concentration  $n_{\text{H}, \text{TS}}$  near the heliospheric shock can be calculated. This value can also be obtained experimentally on the basis of measurements of the backscattered solar Lyman- $\alpha$  emission (for example, onboard SOHO) and the pickup protons onboard *Ulysses*. An analysis of these measurements led to the estimate  $n_{\text{H}, \text{TS}} \sim 0.100 \pm 0.005 \text{ cm}^{-3}$  near *TS*. Comparison of this value with the data of the parametric study leads to a possible range of  $n_{p\infty}$  and  $n_{\text{H}\infty}$  concentrations. This range can be narrowed by invoking astronomical data concerning, firstly, the estimate for the He atom ionization obtained onboard the EUVE<sup>6</sup> along the line of sight toward white dwarfs [45] and, secondly, the value of the He atom concentration  $n_{\text{He}} \sim 0.015 \text{ cm}^{-3}$  [46], obtained by direct measurements onboard *Ulysses*, and its spatial abundance, relative to hydrogen, equal to 0.1. As a result, a relation between  $n_{p\infty}$  and  $n_{\text{H}\infty}$  can be obtained; using this relation, together with the data of parametric study [24], leads to the following most probable estimates of the hydrogen atom and proton concentrations in the local interstellar medium:  $n_{\text{H}\infty} = 0.185 \pm 0.01 \text{ cm}^{-3}$  and  $n_{p\infty} = 0.05 \pm 0.015 \text{ cm}^{-3}$ , which is in agreement with the data of ground-based observations [11].

<sup>6</sup>Extreme Ultraviolet Explorer.

It is interesting to note that the direct measurements of the He velocity and temperature made onboard *Ulysses* [46] showed that the values of these parameters coincide with their values in the local interstellar medium [11], as distinct from the hydrogen parameters which change across the heliospheric interface.

*Filtration of interstellar oxygen and nitrogen atoms.* Onboard the *Ulysses* spacecraft the pickup ions of other chemical elements were also measured. By means of these measurements, data on the cosmic abundance of different elements in the local interstellar medium, independent of astronomical observations, can be obtained using for their interpretation the theoretical description of the process of filtration of different atoms due to charge exchange with outer interface protons (region 3 in Fig. 1 is most efficient for the filtration process). In [47] a comparative analysis of the penetration of interstellar oxygen and nitrogen atoms through this region was made. It was shown that  $81 \pm 2\%$  and  $89 \pm 1\%$  of the interstellar oxygen and nitrogen, respectively, penetrate into the solar system through region 3. Using the calculated filtration coefficient, together with the data of *Ulysses* pickup ion measurements, the oxygen and nitrogen atom concentrations in the local interstellar medium were determined and turned out to be equal to  $n_{\text{OI}\infty} = (7.8 \pm 1.3) \cdot 10^{-5} \text{ cm}^{-3}$  and  $n_{\text{NI}\infty} = (1.1 \pm 0.2) \cdot 10^{-5} \text{ cm}^{-3}$ . Once estimates for the concentrations of different elements have been obtained, their relative cosmic abundances can be evaluated:  $(n_{\text{OI}}/n_{\text{HI}})_{\infty} = (4.3 \pm 0.5) \cdot 10^{-4}$  and  $(n_{\text{NI}}/n_{\text{OI}})_{\infty} = 0.13 \pm 0.01$ . The ratio  $(n_{\text{OI}}/n_{\text{HI}})_{\infty}$  thus obtained is only slightly different from the value  $(4.8 \pm 0.48) \cdot 10^{-4}$  obtained on the basis of spectroscopic observations of absorption lines in stellar spectra [48].

*Summary.* The interaction between the supersonic flow of partially ionized hydrogen plasma of the local interstellar medium and the solar wind produces a complicated flow pattern (Fig. 1) consisting of two shock waves (bow shock *BS* and heliospheric, or termination, shock *TS*) and a tangential discontinuity surface (heliopause *HP*). Due to the charge exchange process, the region between the two shocks (heliospheric interface) separating these supersonic flows plays the role of a filter in the penetration of interstellar H, O, N, and other atoms into the solar system. The best validated model of the phenomenon was developed in [20]. There the interaction of the fully ionized solar-wind hydrogen plasma with the plasma component of the interstellar medium was considered within the framework of continuum mechanics and that with the neutral component (H atoms) within the framework of the kinetic theory, since for hydrogen atoms the Knudsen number based on the main resonance charge exchange process (between H atoms and protons) is  $\text{Kn} \sim 1$ . As shown in this paper, studies within the framework of model [20] and its further development led, firstly, to the prediction of many physical phenomena detected later onboard spacecraft (the discovery of the hydrogen barrier onboard the HST spacecraft, the presence of the interface confirmed, for example, by *Ulysses* measurements, etc.) and, secondly, to the interpretation of previously obtained experimental data (explanation of the Lyman- $\alpha$  absorption spectrum from Sirius in the tail region of the heliosphere obtained onboard HST, interpretation of the backscattered solar radiation anisotropy obtained onboard the SOHO satellite, explanation of the increase in solar proton temperatures at large heliocentric distances measured onboard the *Voyager* spacecraft, etc.). In December 2004 an event awaited for more than 30 years took place, namely, the intersection of the heliospheric shock *TS* by the *Voyager* 1 spacecraft at a distance of 94 a.u., theoretically predicted more than 25 years ago (see, for example, [16, 17]). A special issue of the journal *Science* was devoted to this event (2005, vol. 309, p. 2016).

There are several reasons for the topicality of heliospheric interface research: (1) it is expected that the *Voyager* 1 and 2 spacecraft will transmit information up to the year 2020; (2) in 2008 NASA plans to launch the IBEX spacecraft which will measure the fluxes of energetic neutral atoms arriving from the inner interface at the Earth's orbit; (3) NASA also plans to launch the *Interstellar Probe* spacecraft which in 10 to 15 years will reach distances of the order of 200 a.u.; and (4) the development of technologies which would make it possible to launch a spacecraft to the star nearest to the Sun,  $\alpha$  Centauri, is being planned.

The kinetic-gasdynamic approach to the solution of the problem considered can also be used in other branches of mechanics. Thus, it can be used in problems of disperse medium flows in which the carrier phase can be described within the framework of continuum mechanics, but the applicability of this approach

to the description of the dispersed component interacting with the former is restricted (for example, gas-dust mixtures).

The study was carried out with the support of the Russian Foundation for Basic Research (projects Nos. 04-01-00594 and 04-02-16559), the RFBR-DFG grant No. 03-02-04020, and the Program of Fundamental Research of the Division of Energetics, Machinebuilding, Mechanics, and Control Process of the Russian Academy of Sciences. V. V. Izmodenov also received support from the funds "Dynasty" and "Aid for National Science".

The authors wish to thank A. A. Barmin who read attentively the manuscript and made a number of useful notes.

## REFERENCES

1. E. Parker, "Dynamics of the interplanetary gas and magnetic fields," *Astrophys. J.*, **128**, 664 (1958).
2. K. I. Gringauz, V. V. Bezrukih, V. D. Ozerov, and R. E. Rybchinskii, "Investigation of the interplanetary ionized gas, energetic electrons, and corpuscular solar radiation using three-electrode charged-particle traps onboard the second Soviet space rocket," *Dokl. Akad. Nauk SSSR*, **131**, 1301 (1960).
3. V. N. Zhigulev and E. A. Romishevskii, "Interaction of conducting medium flows with the Earth's magnetic field," *Dokl. Akad. Nauk SSSR*, **127**, 1001 (1959).
4. L. Biermamm, B. Brosowski, and H. Schmidt, "The interaction of the solar wind with a comet," *Solar Physics*, **1**, 254 (1967).
5. V. B. Baranov and M. G. Lebedev, "Self-consistent gasdynamic model of the solar wind flow past a cometary ionosphere with account for the 'mass-loading' effect," *Pisma Astron. Zh.*, **12**, 551 (1986).
6. V. B. Baranov, K. V. Krasnobaev, and A. G. Kulikovskii, "Model of the interaction between the solar wind and the interstellar medium," *Dokl. Akad. Nauk SSSR*, **194**, 41 (1970).
7. G. G. Chernyi, *Introduction to Hypersonic Flow Theory*, Acad. Press, New York (1966).
8. J. L. Bertaux and J. Blamont, "Evidence for a source of an extraterrestrial hydrogen Lyman- $\alpha$  emission: The interstellar wind," *Astron. Astrophys.*, **11**, 200 (1971).
9. G. Thomas and R. Krassa, "OGO-5 measurements of the Lyman- $\alpha$  sky background," *Astron. Astrophys.*, **11**, 218 (1971).
10. C. Weller and R. Meier, "Observations of helium in the interplanetary/interstellar wind: The solar wake," *Astrophys. J.*, **193**, 471 (1974).
11. R. Lallement and P. Bertin, "Northern-hemisphere observations of nearly interstellar gas: possible detection of the local cloud," *Astron. Astrophys.*, **266**, 479 (1992).
12. M. Wallis, "Local interstellar medium," *Nature*, **254**, No. 5497, 202 (1975).
13. V. B. Baranov, M. G. Lebedev, and M. S. Ruderman, "Structure of the region of solar wind — interstellar medium interaction and its influence on H atoms penetrating the Solar System," *Astrophys. Space Sci.*, **66**, 441 (1979).
14. H. W. Ripken and H.-J. Fahr, "Modification of the local interstellar gas properties in the heliospheric interface," *Astron. Astrophys.*, **122**, 181 (1983).
15. J. L. Bertaux, R. Lallement, V. G. Kurt, and E. N. Mironova, "Characteristics of the local interstellar hydrogen determined from Prognoz-5 and 6 interplanetary Lyman-alpha line profile measurements with a hydrogen absorption cell," *Astron. Astrophys.*, **150**, 1 (1985).
16. V. B. Baranov, "Gasdynamics of the solar wind interaction with the interstellar medium," *Space Sci. Rev.*, **52**, 89 (1990).
17. V. B. Baranov, "Gasdynamic model of the local interstellar medium flow past the solar wind. Connection with the experimental data," *Usp. Mekh.*, **1**, No. 1, 3 (2002).
18. E. Parker, "The stellar wind regions," *Astrophys. J.*, **134**, 20 (1961).
19. V. B. Baranov, M. K. Ermakov, and M. G. Lebedev, "Three-component gas-dynamic model of the interaction of the solar wind with the interstellar medium," *Fluid Dynamics*, **17**, No. 5, 754 (1982).
20. V. B. Baranov and Yu. G. Malama, "Model of the solar wind interaction with the local interstellar medium: numerical solution of self-consistent problem," *J. Geophys. Res.*, **98**, No. A9, 15157 (1993).
21. Yu. G. Malama, "Monte Carlo simulation of neutral atom trajectories in the solar system," *Astrophys. Space Sci.*, **176**, 21 (1991).

22. V. B. Baranov, V. V. Izmodenov, and Yu. G. Malama, "On the distribution function of H atoms in the problem of the solar wind interaction with the local interstellar medium," *J. Geophys. Res.*, **103**, No. A5, 9575 (1998).
23. A. V. Myasnikov, D. B. Alexashov, V. V. Izmodenov, and S. V. Chalov, "Self-consistent model of the solar wind interaction with three-component circumsolar interstellar cloud: Mutual influence of thermal plasma, galactic cosmic rays, and H atoms," *J. Geophys. Res.*, **105**, No. A3, 5167 (2000).
24. V. Izmodenov, Yu. Malama, G. Gloeckler, and J. Geiss, "Effects of interstellar and solar wind ionized helium on the interaction of the solar wind with the local interstellar medium," *Astrophys. J. Letters*, **594**, L59 (2003).
25. S. V. Chalov and H.-J. Fahr, "Phase space diffusion and anisotropic pick-up ion distributions in the solar wind: an injection study," *Astron. Astrophys.*, **335**, 746 (1998).
26. D. B. Alexashov, S. V. Chalov, A. V. Myasnikov, V. V. Izmodenov, and R. Kallenbach, "The dynamical role of the anomalous cosmic rays in the outer heliosphere," *Astron. Astrophys.*, **420**, 729 (2004).
27. D. B. Alexashov, V. B. Baranov, E. V. Barskii, and A. V. Myasnikov, "Axisymmetric magnetohydrodynamic model of the interaction between the solar wind and the interstellar medium," *Pisma Astron. Zh.*, **26**, 862 (2000).
28. V. V. Izmodenov, D. B. Alexashov, and A. V. Myasnikov, "Direction of the interstellar H atom inflow in the heliosphere: Role of the interstellar magnetic field," *Astron. Astrophys.*, **437**, L35 (2005).
29. R. Lallement, E. Quémerais, J. L. Bertaux, S. Ferron, D. Kotroumpa, and R. Pellinen, "Deflection of the interstellar neutral hydrogen flow across the heliospheric interface," *Science*, **307**, No. 5714, 1447 (2005).
30. P. R. Gazis, "Solar cycle variation in the heliosphere," *Rev. Geophys.*, **34**, 379 (1996).
31. V. B. Baranov and N. A. Zaitsev, "On the problem of the heliospheric interface response to the cycles of the solar activity," *Geophys. Res. Lett.*, **25**, 4051 (1998).
32. C. Wang and J. Belcher, "The heliospheric boundary response to large-scale solar wind fluctuations: A gasdynamic model with pickup ions," *J. Geophys. Res.*, **104**, No. A1, 549 (1999).
33. V. V. Izmodenov and Yu. G. Malama, "Variations of interstellar H atom parameters in the outer heliosphere: solar cycle effects," *Adv. Space Res.*, **34**, 74 (2004).
34. V. V. Izmodenov, Yu. G. Malama, and M. S. Ruderman, "Solar cycle influence on the interaction of the solar wind with Local Interstellar Cloud," *Astron. Astrophys.*, **429**, 1069 (2005).
35. V. V. Izmodenov and D. B. Alexashov, "Model of the tail region of the heliospheric interface," *Pisma Astron. Zh.*, **29**, 69 (2003).
36. Yu. G. Malama, V. V. Izmodenov, and S. V. Chalov, "Modeling of the heliospheric interface: multi-component nature of the heliospheric plasma," *Astron. Astrophys.*, **445**, 693 (2006).
37. G. P. Zank, H. L. Pauls, L. L. Williams, and D. T. Hall, "Interaction of the solar wind with the local interstellar medium: a multifluid approach," *J. Geophys. Res.*, **101**, No. A10, 21639 (1996).
38. D. B. Alexashov and V. V. Izmodenov, "Kinetic vs multi-fluid models of the heliospheric interface: a comparison," *Astron. Astrophys.*, **439**, 1171 (2005).
39. V. V. Izmodenov, M. A. Gruntman, and Yu. G. Malama, "Interstellar hydrogen atom distribution function in the outer heliosphere," *J. Geophys. Res.*, **106**, 10681 (2001).
40. V. B. Baranov, M. G. Lebedev, and Yu. G. Malama, "The influence of the interface between heliosphere and the local interstellar medium on the penetration of the H atoms to the solar system," *Astrophys. J.*, **375**, 347 (1991).
41. J. L. Linsky and B. E. Wood, "The  $\alpha$  Centauri line of sight: D/H ratio, physical properties of local interstellar gas and measurements of heated hydrogen at heliospheric interface," *Astrophys. J.*, **463**, 254 (1996).
42. J. L. Linsky, "GHRS observations of the LISM," *Space Sci. Rev.*, **78**, 157 (1996).
43. B. E. Wood, J. L. Linsky, and G. P. Zank, "Heliospheric, astrospheric, and interstellar Ly- $\alpha$  absorption toward 36Ophiuchi," *Astrophys. J.*, **537**, 304 (2000).
44. V. V. Izmodenov, R. Lallement, and Yu. G. Malama, "Heliospheric and astrospheric hydrogen absorption toward Sirius: No need for interstellar hot gas," *Astron. Astrophys.*, **342**, L13 (1999).
45. B. Wolff, D. Koester, and R. Lallement, "Evidence for an ionization gradient in the local interstellar medium: EUVE observations of white dwarfs," *Astron. Astrophys.*, **346**, 969 (1999).
46. M. Witte, "Kinetic parameters of interstellar neutral helium. Review of results obtained during one solar cycle with the Ulysses/GAS-instrument," *Astron. Astrophys.*, **426**, 835 (2004).
47. V. V. Izmodenov, Yu. G. Malama, G. Gloeckler, and J. Geiss, "Filtration of interstellar H, O, N atoms through the heliospheric interface: Inferences on local interstellar abundances of the elements," *Astron. Astrophys.*, **414**, L29 (2004).
48. J. L. Linsky, A. Dipas, B. E. Wood, *et al.*, "Deuterium and the local interstellar medium properties for the Procyon and Capella lines of sight," *Astrophys. J.*, **476**, 366 (1995).